Delay-Constrained Energy Optimization in High-Latency Sensor Networks

Poongovan Ponnavaikko, *Member, IEEE*, Sarah Kate Wilson, *Fellow, IEEE*, Milica Stojanovic, *Fellow, IEEE*, JoAnne Holliday, *Member, IEEE*, and Kamal Yassin, *Member, IEEE*

***Abstract*— Sensor networks deployed in high-latency environments, such as underwater acoustic and satellite channels, find critical applications in disaster prevention and tactical surveillance. The sensors in these networks have limited energy reserves. In order to extend the lifetime of these sensors, energy must be conserved in all layers of the protocol stack. In addition to long propagation delays, these channels are characterized by limited bandwidth and a lack of well-established closed-form analytical models. This fact makes finding cross-layer energy-optimal solutions a difficult problem to solve. Our goal is to compute near-optimal routes, schedules and transmit power levels for delay-constrained applications of high-latency sensor networks. We present a mixed-integer programming relaxation of the optimization problem. We further propose a decentralized algorithm to iteratively solve the relaxed optimization problem. Comparative simulation analysis shows that our decentralized approach is approximately 3∼6 dB more energy-efficient and 2∼5 dB more throughput-efficient than the heuristic, time-sensitive greedy forwarding, and least-cost routing algorithms.**

***Index Terms*— Cross-layer energy optimization, high-latency sensor networks, underwater acoustic medium, delay-intolerant applications, large propagation delays, decentralized algorithm.**

I. Introduction

UNDERWATER acoustics and satellite-based long-range radio frequency (RF) channels are examples of physical communication media used in high-latency sensor network (HLSN). In this paper, we focus on cross-layer energy optimization for time-sensitive applications over HLSN. These sensor networks are envisioned to enable a wide-ranging set of time-sensitive civilian and military applications. Examples of such applications include disaster prevention, tactical distributed surveillance, military target detection, oil-spill monitoring, coastline protection, and early warning systems for earthquakes and tsunamis [1], [2]. The sensor nodes in these networks collaboratively collect and relay telemetry data to centralized sink nodes. Fig.1 shows such a sensor network in a three-dimensional (3D) underwater environment. These sensors are powered by batteries that are both difficult and expensive to replace or recharge after deployment. Hence minimizing energy usage across all layers in the protocol stack becomes essential for such networks.

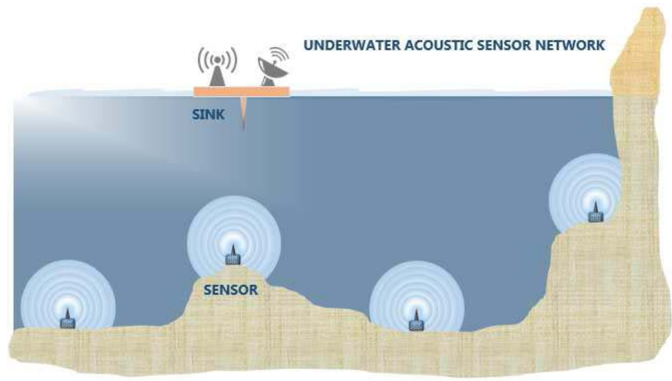

Fig. 1. Underwater acoustic sensor network.

The inherent characteristics of the physical medium used in these networks pose significant challenges to the design of sensor networks for delay-intolerant applications. In addition to long and variable propagation delays, these networks have limited bandwidth, severe multipath fading, and large Doppler spreads. This results in a poor link quality with high error rates [3], [4].

Our goal is to compute time-constrained energy-optimal routes, schedules, and power levels for a time-slotted HLSN. In terrestrial RF networks, for a given distance, the energy consumption can be modeled as a convex function of the number of transmitted bits and the transmit time [5]. Analyzing the convexity of such a function for HLSN is generally difficult due to the lack of well-established closed-form analytical models [3], [6]. This fact makes the cross-layer energy-optimization problem for HLSN difficult to solve.

Our approach to finding a near-optimal solution involves relaxing the nonconvex optimization problem by using piecewise-linear approximations of the channel's power-rate function. This allows us to reformulate our problem into an mixed-integer programming (MIP) problem which can be solved using standard methods. This reformulation allows us to compute near-optimal routes, schedules, and power control solutions for HLSN. We also propose a sub-optimal, but more practical distributed algorithm to solve our optimization problem. The near-optimal solutions obtained from our centralized

Manuscript received November 30, 2016; accepted April 25, 2017. Date of publication May 11, 2017; date of current version June 12, 2017. This paper was presented at the IEEE GLOBECOM, 2013, Atlanta, GA, USA. The associate editor coordinating the review of this paper and approving it for publication was Dr. Roozbeh Jafari. *(Corresponding author: Poongovan Ponnavaikko.)*

P. Ponnavaikko and J. Holliday are with the Computer Engineering Department, Santa Clara University, CA 95053 USA (e-mail: pponnavaikko@scu.edu; jholliday@scu.edu).

S. K. Wilson is with the Electrical Engineering Department, Santa Clara University, CA 95053 USA (e-mail: skwilson@scu.edu).

M. Stojanovic is with the Electrical and Computer Engineering Department, Northeastern University, Boston, MA 02115 USA (e-mail: millitsa@ece.neu.edu).

K. Yassin was with the Electrical Engineering Department, Santa Clara University, CA 95053 USA. He is now with ASSIA, Inc., Redwood City, CA 94065 USA (e-mail: kyassin@gmail.com).

Digital Object Identifier 10.1109/JSEN.2017.2703639

approach gives us a benchmark for comparing the performance of our distributed approach against.

In our decentralized approach, the individual sensors cooperate with each other to iteratively solve the optimization problem. We decompose our centralized MIP problem into subproblems that are localized to each of the sensors. At each iteration, the sensors solve the subproblem and then exchange their results with neighboring sensors. Each of the sensors then revises its subproblem based on the new information about its neighbors' utility. This is repeated until the results of the subproblems converge.

Our main contributions are two-fold. We find a centralized solution to minimizing energy for HLSN by reformulating a nonconvex problem into one that can be solved more easily. We then find a more practical decentralized version of this algorithm by decomposing the centralized problem into subproblems that the sensors can solve iteratively. We compare the performance of our centralized and decentralized algorithms to that of alternative approaches such as time-sensitive greedy forwarding (TGF) and time-sensitive least cost routing (TLCR) as described in Sections VII-D.1 and VII-D.2, respectively.

In our preliminary work [7], we proposed a centralized routing and power control algorithm using an MIP relaxation of the delay-constrained energy optimization problem. Here we extend that approach by updating our optimization problem to additionally produce time division multiple access (TDMA) schedules. Further, we also present a decentralized version of our algorithm.

This paper is organized as follows: Section II discusses the related work in this area of research. In Section III, we give an overview of the system model. We then present a centralized routing, scheduling, and power control algorithm in Sections IV and V. In Section VI, we propose a decentralized version of our algorithm. Section VII explains our test setup and analyzes the results. Finally, in Section VIII, we present our concluding remarks.

II. Related Work

Cross-layered energy optimization in terrestrial RF sensor networks is a heavily researched topic [8]. The methods from those studies are generally not feasible in HLSN due to its fundamentally different channel characteristics. In recent years much attention has been paid to energy optimization in underwater acoustic sensor network (UWA-SN).

Crucial insights into the physical layer design considerations of an acoustic medium are provided by [9]. Packet retransmissions are expensive in UWA-SN due to its large propagation delays. As a result, focus at the data-link layer has been on designing protocols that proactively avoid collisions and are cognizant of the long propagation delays. A modified version of the ALOHA protocol that uses energy as the main performance metric instead of the bandwidth, is proposed in [10]. In paper [11], they suggest a medium access control (MAC) protocol that uses both schedules and handshakes to avoid collisions. A TDMA-based protocol that increases channel use by taking advantage of the long propagation delays is discussed in [12]. While these papers focus on the data-link layer, the protocols could be integrated with network and physical layer solutions to further minimize overall energy use.

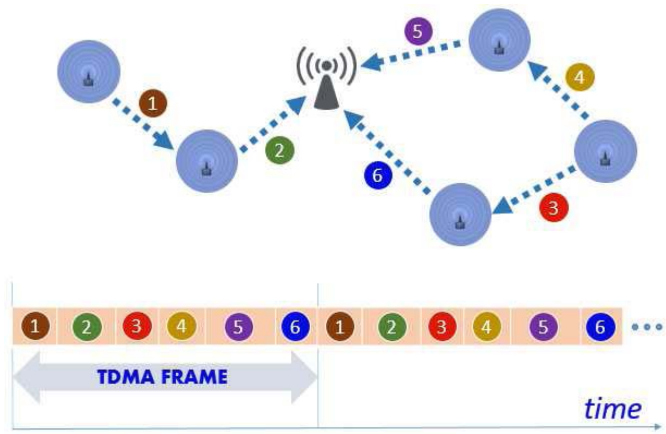

Fig. 2. Sensor Network with TDMA scheduling.

Several papers have looked into network layer energy optimization for UWA-SN. A routing protocol that dynamically re-configures its routes based on the residual energy of the nodes is proposed in [13]. In [14] the authors suggest a routing approach that conserves energy by minimizing the number of required packet re-transmissions for delay-sensitive applications. An analysis on the optimum number of hops and transmission trials in terms of energy consumption, is presented in [15]. A routing algorithm proposed in [16] makes online routing decisions to minimize energy consumption while meeting end to end error rate and delay requirements.

Both [14] and [16] use path-specific delay constraints for meeting differentiated quality of service (QoS) requirements for packets from a given node to the sink. In this paper, we consider a global TDMA schedule where every link is assigned slots in each frame such that data from all nodes in the network reach the sink in one frame period. Also, the algorithms discussed in the above papers are designed to work with an interference-limited code division multiple access (CDMA) based MAC protocol. In this paper, we consider a slotted TDMA based MAC scheme since avoiding collisions is one way to minimize energy consumption. Further, it also allows us to make good use of the propagation delays.

III. System Overview

We consider a generic HLSN model where a number of stationary sensor nodes are arbitrarily deployed in a 3D environment. Each of the sensors collects time-sensitive data and collaborate amongst themselves to relay their traffic to the sink nodes where the data is processed. The sensor nodes have limited energy reserves. They are capable of full-duplex communication and can buffer data until the link is available for transmission. Fig.2 shows such a network with a number of sensor nodes dispersed over a large area. A reasonable range for a sensor in UWA-SN is $2 - 10\,\text{kms}$, so it is realistic to have 10 to 30 nodes in an area of $100\,\text{km}^2$ [17].

In setting up our model, the only assumptions that we make about the physical medium of the network is that it exhibits large propagation delays. This differs from terrestrial RF networks where the transmit time of a signal dominates its propagation time. As a result, both transmission and propagation delays need to be taken into account while designing algorithms to compute transmission schedules for HLSN. The sensors are capable of adjusting their transmit power level within a predetermined range, to achieve a desired signal-to-noise ratio (SNR) for a link. In cases where packets are corrupted and unrecoverable by forward error correction (FEC), the sensors cooperatively handle the retransmission of the packet.

For the data link layer, we consider a slotted synchronous TDMA scheme with a periodic schedule. The schedule has a maximum frame duration T which is divided into multiple time slots. Each of the links in the network is allocated a variable number of time slots. This is illustrated in Fig.2. Data sent by the sensors to the sink could get load balanced over multiple outgoing links. We consider a link between two sensors to be feasible if its SNR is above a predefined threshold and if the destination node is geographically closer to a sink than the source.

In our system model, we parameterize the size of the network, the number and location of each of the nodes, the system load, the desired bit error rate (BER) for the links and the maximum time period for the TDMA frame. We shortlist a set of candidate next hop nodes for each of the sensors. We also identify all pairs of links that could potentially interfere with each other, so we can avoid scheduling conflicts. We then formulate a time-constrained optimization problem to minimize the overall energy consumption while increasing the throughput efficiency of the network. The output of the problem would be the selected set of outgoing links for each of the sensors, their power levels, their load distributions, their schedules and the minimum required size of the TDMA frame, T_{min}.

IV. Time-Constrained Energy Optimization Formulation

Let $\mathcal{V}$ be the set of all sensor nodes and $\mathcal{L}$ be the set of all feasible links in the network. For every sensor node υ, let h_υ denote the amount of data that node υ generates in one time period T. Let ρ_l be the relay processing power, which is the power required by the relay sensor to process incoming traffic on link l. Let $\mathcal{O}_\upsilon$ and $\mathcal{I}_\upsilon$ be the set of all outgoing and incoming links for node υ. For every link $l \in \mathcal{L}$, let w_l, p_l, e_l, t_l, τ_l and r_l represent the number of transmitted bits, transmit power, energy consumed, allocated transmit time, propagation time and the transmit rate, respectively. Let $\mathrm{x}(l)$ and $\mathrm{r}(l)$ be the source and destination nodes of link l. Let the function $\mathcal{P}_l(r_l)$ represent power-rate relationship for link l, ie., $p_l = \mathcal{P}_l(r_l)$ is the transmission power required to achieve a transmit rate of r_l for link l.

The delay-constrained energy-optimal routes, power levels, transmit rates and transmit times can be found by solving the following optimization problem given in Eqs. (1)-(3) [5].

$$\text{minimize} \quad \sum_{l\in\mathcal{L}} \left(\mathcal{P}_l\left(\frac{w_l}{t_l}\right) + \rho_l\right) t_l \tag{1}$$

$$\text{subject to} \quad \sum_{l\in\mathcal{L}} (t_l + \tau_l) \le T \tag{2}$$

$$\sum_{l\in\mathcal{O}_\upsilon} w_l - \sum_{m\in\mathcal{I}_\upsilon} w_m = h_\upsilon, \quad \forall\, \upsilon \in \mathcal{V} \tag{3}$$

The minimization objective function, Eq. (1), is the sum total of energy consumed on every link in the network. The delay constraint, Eq. (2), specifies an upper bound on the sum total of the allocated transmit time and the propagation time of all the links. The flow conservation constraints, Eq. (3), ensure that the data generated by all the sensors are accounted for and that they flow towards and eventually terminate at a sink node. For every sensor, the total data transmitted on all its outgoing links is equal to the sum of the data generated by the sensor and the total data received on all its incoming links. While the constraints in the above problem are linear, the $\mathcal{P}_l(w_l/t_l)\, t_l$ term in the objective function is nonlinear. It is a function of a nonlinear combination of two variables and its convexity with respect to w_l and t_l is unknown. It represents e_l, the energy consumed on link l. Table I summarizes the definitions of all the symbols used in this paper.

A. Scheduler Constraints

The constraint Eq. (2) allows for collision free transmissions. It reserves enough time slots per link to cover not only the time required to transmit the signal but also for it to propagate to its intended destination. Given *a priori* knowledge of the link propagation delays, the acoustic channels could be better used by overlapping the schedules without causing any conflicts at the receiving nodes [12]. Overlapping transmissions in this manner results in an increased network throughput as is illustrated in Fig.3.

Our goal is to formulate the delay-constrained energy optimization problem to solve for transmission schedules in addition to routes and power levels. A periodic TDMA schedule for a link is defined by its transmit start time relative to the beginning of the frame and the length of time allocated to it. The constraints need to ensure that the transmissions on a link do not interfere with any other link, whether in the same TDMA frame or in subsequent ones. They must also ensure that the transmissions complete within the same TDMA frame that they were initiated in.

A pair of links could interfere with each other if the destination node of either of the links is in the interference range of the source node of the other. Scheduling constraints need to be setup for every pair of interfering links in the network, including those that originate from the same source.

Let s_l be a continuous variable that denotes the time relative to the start of the frame when link l is scheduled to start transmitting for t_l seconds. Let ψ_l be the set of all links that can interfere with link l. Let $d_{u\upsilon}$ be the distance between nodes u and υ. Let $d_l = d_{\mathrm{x}(l)\mathrm{r}(l)}$ and $\tau_l = \tau_{\mathrm{x}(l)\mathrm{r}(l)}$. Let τ_{max} be the maximum time required for the signal to propagate

TABLE I
SYMBOL DESCRIPTIONS

SYMBOL	DESCRIPTION
T	TDMA time period
$\mathcal{V}$	Set of all nodes in the network
$\mathcal{L}$	Set of all links in the network
$\mathcal{I}_v$	Set of all ingress links of node v
$\mathcal{O}_v$	Set of all egress links of node v
l_{uv}	A link from node u to node v
h_v	Data generated by node v in time T
ρ_l	Relay processing power for link l
d_l, d_{uv}	Link distance
p_l	Power level used in link l
e_l	Energy consumed in link l
s_l	Transmit start time for link l
t_l	Transmit time allocated for link l
r_l	Transmit data rate of link l
w_l	Size of the data to be sent on link l
τ_l	Propagation time for link l
τ_{max}	Maximum propagation time
$\mathtt{x}(l)$, $\mathtt{r}(l)$	Source and destination nodes of link l
$\hat{r}_l$	Approximation of $\log(r_l)$
λ_w^v	Flow constraint's Lagrange multiplier
λ_s^{lm}	Schedule constraint's Lagrange multiplier
$\mathcal{P}_l(r_l)$	Power vs. rate function for link l
$\mathbb{P}_l(\hat{r}_l)$	log-power vs. log-rate function for link l
ψ_l	Set of all links interfering with link l
$\mathscr{L}$, $\mathscr{D}$	Lagrange and the dual objective functions
o_{uv}	Relative priority between nodes u and v
c_s	Propagation speed of the signal
ϵ	Bit error rate
t_l^{ub}, t_l^{lb}	Bounds for the link transmit time
T_{min}	Minimum required TDMA frame size
B_{lm}	Schedule constraint's bound for a link pair
$\tilde{f}(x)$	Piecewise-linear approximation of $f(x)$
$\mathcal{C}_l(w_l, s_l, t_l)$	Objective for the link-specific subproblem
α_i, β_i	Step sizes for the subgradient algorithm
$g_{\lambda_w^v}$, $g_{\lambda_s^{lm}}$	Subgradients of the dual function

beyond the interference range of the sensor nodes. Let o_{uv} be a binary variable that prioritizes the order in which nodes transmit within a frame. If o_{uv} is set to 1, then node u transmits before node v, and vice versa.

As part of the staggered TDMA underwater MAC protocol (STUMP) introduced in [12], the authors present the following set of constraints between two links l and m to prevent a collision at either of their destination nodes.

$$\begin{aligned} t_l + \tau_l - \tau_{\mathtt{x}(m)\mathtt{r}(l)} - T \\ \leq s_m - s_l - o_{\mathtt{x}(l)\mathtt{x}(m)}T \\ \leq -t_m + \tau_l - \tau_{\mathtt{x}(m)\mathtt{r}(l)} \end{aligned} \tag{4}$$

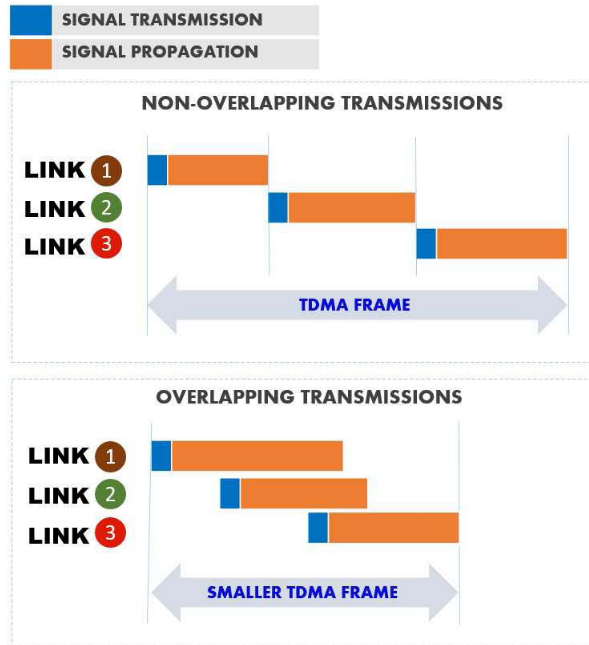

Fig. 3. Increased channel use with overlapping TDMA schedules.

In this paper, we extend the STUMP constraints by making use of the symmetry between their lower and upper bounds. We derive a single constraint that can be set up at link $l \in \mathcal{L}$, for every link $m \in \psi_l$ that falls within its interference range. We set o_{uv} to 1, if node v is closer to a sink than the node u, indicating that node u gets to transmit before node v in the frame.

Given that $o_{uv} = 1 - o_{vu}$, the constraints in Eq. (4) can be rewritten as follows $\forall\, l \in \mathcal{L},\ m \in \psi_l$:

$$\begin{aligned} s_l - s_m + t_l \leq \ & \tau_{\mathtt{x}(m)\mathtt{r}(l)} - \tau_l \\ & + o_{\mathtt{x}(m)\mathtt{x}(l)}T \end{aligned} \tag{5}$$

$$\begin{aligned} s_m - s_l + t_m \leq \ & \tau_l - \tau_{\mathtt{x}(m)\mathtt{r}(l)} \\ & + o_{\mathtt{x}(l)\mathtt{x}(m)}T \end{aligned} \tag{6}$$

Using change of variables, Eq. (6) can equivalently be written as follows $\forall\, m \in \mathcal{L},\ l \in \psi_m$:

$$\begin{aligned} s_l - s_m + t_l \leq \ & \tau_m - \tau_{\mathtt{x}(l)\mathtt{r}(m)} \\ & + o_{\mathtt{x}(m)\mathtt{x}(l)}T \end{aligned} \tag{7}$$

From Eqs. (6) and (7), we note that two constraints get added for every pair of potentially interfering links. Both the constraints set an upper bound on $s_l - s_m + t_l$. We combine the two constraints in Eqs. (5) and (7) by using the tighter upper bound as follows:

$$t_l + s_l - s_m \leq B_{lm}, \quad \forall\, l \in \mathcal{L},\ m \in \psi_l \tag{8}$$

$$\begin{aligned} \text{where, } B_{lm} = \min \begin{pmatrix} \left(\tau_{\mathtt{x}(m)\mathtt{r}(l)} - \tau_l\right), \\ \left(\tau_m - \tau_{\mathtt{x}(l)\mathtt{r}(m)}\right) \end{pmatrix} \\ + o_{\mathtt{x}(m)\mathtt{x}(l)}T \end{aligned} \tag{9}$$

In addition to the scheduler constraints in Eq. (8), we need the following set of per-link constraints defined in Eq. (10). They ensure that the transmission on every link propagates

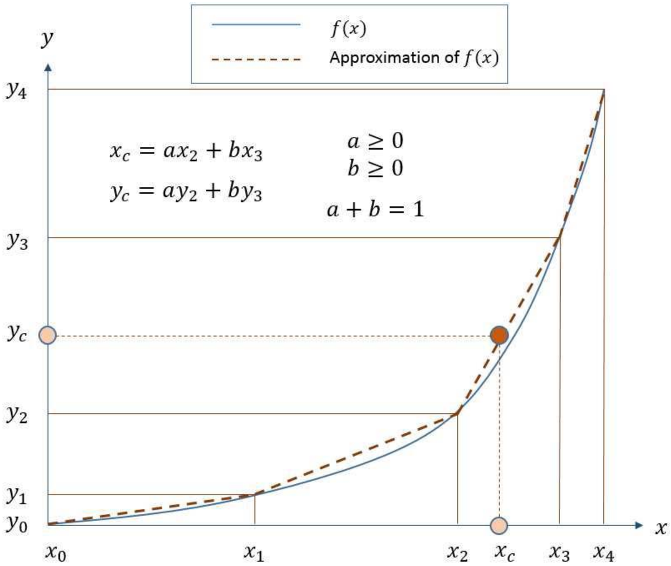

Fig. 4. Piecewise-linear approximation of $f(x)$.

beyond its interference range before the time period of the frame expires.

$$s_l + t_l \leq T - \tau_{max}, \quad \forall\, l \in \mathcal{L} \tag{10}$$

The above constraints in Eq. (10) prevent the transmissions initiated in one frame from causing an interference in a subsequent time frame. They also ensure that transmissions on all links in the network complete within the specified time period T. Unlike Eq. (2), our updated scheduler constraints, Eqs. (8, 10) together allow multiple links to get scheduled simultaneously without causing conflicts. We hence replace Eq. (2) with Eqs. (8) and (10) in our optimization problem.

The maximum frame size, T, is an input parameter to our optimization problem that solves for conflict-free overlapping schedules. The minimum size of the TDMA frame, T_{min}, that is required to realize the generated schedules, is computed as $T_{min} = \max\{s_l + t_l + \tau_{max} \mid \forall l \in \mathcal{L}\}$.

V. Relaxing the Optimization Problem

We begin by substituting the nonlinear term in the objective function, Eq. (1), with the variable e_l which represents the energy consumed on link l. We then add linear constraints to establish the relationship between $\log(e_l)$, $\log(w_l)$ and $\log(t_l)$, where log represents the logarithmic function. Since $e_l = \mathcal{P}_l\,(w_l/t_l)\,t_l$, we have that:

$$\log(e_l) = \log\left(\mathcal{P}_l\left(\frac{w_l}{t_l}\right)\right) + \log(t_l) \tag{11}$$

Let $\mathbb{P}_l$ represent the relationship between $\log(p_l)$ and $\log(r_l)$ such that, $\log(p_l) = \mathbb{P}_l(\log(r_l))$. Then we have:

$$\log(e_l) = \mathbb{P}_l(\log(w_l) - \log(t_l)) + \log(t_l) \tag{12}$$

We now use the piecewise-linear approximations of functions $\mathbb{P}_l$ and log to formulate our MIP problem. As illustrated in Fig.4, let $\tilde{f}(x)$ represent a piecewise-linear approximation of the function $f(x)$. Let $\hat{r}_l$ represent an approximation of $\log(r_l)$. Then, the MIP relaxed-optimization problem can be written as:

$$\text{minimize} \quad \sum_{l\in\mathcal{L}} (e_l + \rho_l t_l) \tag{13}$$

$$\text{subject to} \quad \sum_{l\in\mathcal{O}_v} w_l - \sum_{m\in\mathcal{I}_v} w_m = h_v, \ \forall\, v \in \mathcal{V} \tag{14}$$

$$t_l + s_l - s_m \leq B_{lm}, \ \forall\, l \in \mathcal{L},\ m \in \psi_l \tag{15}$$

$$s_l + t_l \leq T - \tau_{max}, \ \forall\, l \in \mathcal{L} \tag{16}$$

$$\hat{r}_l = \tilde{\log}(w_l) - \tilde{\log}(t_l), \ \forall\, l \in \mathcal{L} \tag{17}$$

$$\tilde{\log}(e_l) = \tilde{\mathbb{P}}_l(\hat{r}_l) + \tilde{\log}(t_l), \ \forall\, l \in \mathcal{L} \tag{18}$$

The objective function in Eq. (13) is the same as Eq. (1), but with the nonlinear term $\mathcal{P}_l\,(w_l/t_l)\,t_l$, replaced with the variable e_l. The rate constraints in Eq. (17) establish the relationship between variables that represent the transmit rate, bits transmitted and transmit time. Similarly, the energy constraints in Eq. (18) establishes the relationship between the variables that represent the energy consumed, transmit power and the transmit time.

VI. Decentralized Cooperative Optimization

The computational complexity of the centralized algorithm increases with the number of nodes in the network. A decentralized approach where the nodes communicate with their neighbors and locally compute network solutions, is inherently more scalable. We propose a decomposition of our MIP problem into subproblems that can then be solved iteratively in a distributed manner.

Our problem formulation exclusively uses link-specific variables. So, our approach involves separating it into $|\mathcal{L}|$ subproblems, one for each of the links in the network. Our objective function is already separable in functions of variables that belong to the same link. Complicating constraints that involve variables associated with more than one link, prevent a straightforward decomposition of our problem. Simple constraints on the other hand are directly separable. We use *Lagrange relaxation* to move the complicating constraints to the objective function after assigning it with weights *(Lagrange multipliers)*. The weights represent a penalty for violating the corresponding constraint [18, p. 1668]. This relaxation allows us to decompose our optimization problem into link-specific subproblems.

For a given vector of multipliers, the optimal value of the relaxed problem provides a lower bound on the optimal value of the original problem, also called the *primal problem*. Finding values for the multipliers that get us the best lower bound, is called the *Lagrange dual* problem. We solve the Lagrange dual problem iteratively using the *subgradient method*, where the multipliers are adjusted at every iteration based on the degree of the constraint violations.

Duality gap is the absolute difference between the primal and dual solutions. When the duality gap is zero, a feasible and optimal primal solution can be recovered from the dual optimal solution. For an MIP problem like ours, the duality gap is non-zero in general. As a result, the iterative subgradient algorithm does not guarantee the convergence of the solution to our primal problem. Hence we use a convex combination of solutions generated at all iterations. This is known to converge to the optimal solution of the integral-relaxed primal problem [19]. Finally, we employ a heuristic algorithm, seeded by the values for the primal variables thus obtained, to find feasible solutions to our original problem.

A. Decomposition Into Subproblems

We start by identifying Eqs. (14) and (15) as the complicating constraints in our MIP problem, since they use variables associated with more than one link. The remaining constraints viz., Eqs. (16), (17) and (18) are easily separable. We use Lagrange relaxation to move the complicating constraints weighted with Lagrange multipliers, into the problem objective.

Let λ_w^v and λ_s^{lm} be the Lagrange multipliers associated with constraints in Eqs. (14) and (15) respectively. We then get the following Lagrange function $\mathscr{L}$:

$$\begin{aligned}\mathscr{L}(\boldsymbol{w}, \boldsymbol{s}, \boldsymbol{t}, \boldsymbol{\lambda_w}, \boldsymbol{\lambda_s}) &= \sum_{l\in\mathcal{L}} (e_l + \rho_l t_l) \\ &+ \sum_{v\in\mathcal{V}} \lambda_w^v \left(\sum_{l\in\mathcal{O}_v} w_l - \sum_{l\in\mathcal{I}_v} w_l - h_v \right) \\ &+ \sum_{l\in\mathcal{L}} \sum_{m\in\psi_l} \lambda_s^{lm} (t_l + s_l - s_m - B_{lm}) \end{aligned} \tag{19}$$

$$\begin{aligned}\text{where,}\quad \boldsymbol{w} &= [w_l,\ l\in\mathcal{L}] \quad \boldsymbol{\lambda_w} = \left[\lambda_w^v,\ v\in\mathcal{V}\right] \\ \boldsymbol{s} &= [s_l,\ l\in\mathcal{L}] \quad \boldsymbol{\lambda_s} = \left[\lambda_s^{lm},\ l\in\mathcal{L},\ m\in\psi_l\right] \\ \boldsymbol{t} &= [t_l,\ l\in\mathcal{L}] \end{aligned} \tag{20}$$

While $\boldsymbol{\lambda_s} \geq 0$, $\boldsymbol{\lambda_w}$ is not restricted in sign since they are associated with an equality constraint. In our network, λ_w^v is a per-node variable and is associated with node v, whereas the λ_s^{lm}, $\forall m \in \psi_l$ multipliers are maintained at link l.

The dual function $\mathscr{D}$, can then be obtained by minimizing the Lagrangian over the primal variables [18, p. 1669].

$$\mathscr{D}(\boldsymbol{\lambda_w}, \boldsymbol{\lambda_s}) = \underset{(\boldsymbol{w},\boldsymbol{s},\boldsymbol{t})}{\text{minimize}} \ \mathscr{L}(\boldsymbol{w}, \boldsymbol{s}, \boldsymbol{t}, \boldsymbol{\lambda_w}, \boldsymbol{\lambda_s})$$

The dual function is concave function of the Lagrange multipliers, even though our primal problem is nonconvex. By regrouping the relevant terms, the dual function $\mathscr{D}$ gets decomposed into subproblems for each of the links.

$$\begin{aligned}\mathscr{D}(\boldsymbol{\lambda_w}, \boldsymbol{\lambda_s}) &= \sum_{l\in\mathcal{L}} \left[\underset{(w_l,s_l,t_l)}{\text{minimize}} \ \mathcal{C}_l(w_l, s_l, t_l) \right] \\ &- \sum_{v\in\mathcal{V}} \lambda_w^v h_v - \sum_{l\in\mathcal{L}} \sum_{m\in\psi_l} \lambda_s^{lm} B_{lm} \end{aligned} \tag{21}$$

$$\begin{aligned}\text{where,}\quad &\mathcal{C}_l(w_l, s_l, t_l) \\ &= e_l + \left(\lambda_w^{\mathtt{x}(l)} - \lambda_w^{\mathtt{r}(l)}\right) w_l \\ &+ \left(\sum_{m\in\psi_l} \left(\lambda_s^{lm} - \lambda_s^{ml}\right) \right) s_l + \left(\sum_{m\in\psi_l} \lambda_s^{lm} + \rho_l \right) t_l \end{aligned} \tag{22}$$

Since Eq. (22) only involves variables associated with one link, $\mathcal{C}_l(w_l, s_l, t_l)$ can be minimized locally.

For a given vector of values for $\boldsymbol{\lambda_w}$ and $\boldsymbol{\lambda_s}$, the dual function $\mathscr{D}$, is a lower bound for the optimal value of the original problem. The best lower bound can then be obtained by solving the following dual optimization problem:

$$\begin{aligned} &\text{maximize} \quad \mathscr{D}(\boldsymbol{\lambda_w}, \boldsymbol{\lambda_s}) \\ &\text{subject to} \quad \boldsymbol{\lambda_s} \geq 0 \end{aligned} \tag{23}$$

B. Iterative Subgradient Optimization

The dual optimization problem, Eq. (23), can be solved iteratively in a distributed manner using the projected subgradient method. At every iteration, the current value of the multipliers is used to compute the dual function by solving the subproblems. The multiplier values are then updated along the subgradient direction according to a prescribed sequence of step lengths.

At iteration i of the subgradient algorithm, the following MIP subproblem is solved for all links $l \in \mathcal{L}$:

$$\underset{(w_l,s_l,t_l)}{\text{minimize}} \quad \mathcal{C}_l(w_l, s_l, t_l) \tag{24}$$

$$\text{subject to} \quad s_l + t_l \leq T - \tau_{max} \tag{25}$$

$$\hat{r}_l = \tilde{\log}(w_l) - \tilde{\log}(t_l) \tag{26}$$

$$\tilde{\log}(e_l) = \tilde{\mathbb{P}}_l\left(\hat{r}_l\right) + \tilde{\log}(t_l) \tag{27}$$

$$w_l \geq 0, \quad s_l \geq 0, \quad t_l \geq 0 \tag{28}$$

Appendix VIII explains our modeling of the above subproblem, Eqs. (24)-(28), in further detail.

Using the primal values $(\boldsymbol{w}, \boldsymbol{s}, \boldsymbol{t})$ thus obtained, we can compute the subgradients of the dual function at $(\boldsymbol{\lambda_w}, \boldsymbol{\lambda_s})$ as follows:

$$g_{\lambda_w^v} = \sum_{l\in\mathcal{O}_v} w_l - \sum_{l\in\mathcal{I}_v} w_l - h_v \tag{29}$$

$$g_{\lambda_s^{lm}} = t_l + s_l - s_m - B_{lm} \tag{30}$$

The primal solutions of the subproblems computed at link l is then shared with the link source node $\mathtt{x}(l)$, link destination node $\mathtt{r}(l)$ and with all links $m \in \psi_l$, that fall within the interference range of link l. Let $\{\alpha_i\}$ and $\{\beta_i\}$ be sequences of positive harmonic step sizes that are square summable but not summable, eg. $a/a+bi$ where $a \geq 0, b \geq 0$ [20]. The Lagrange multiplier λ_w^v is then updated at node v using the primal solutions from all the incoming and outgoing links, as follows:

$$\lambda_w^v(i+1) = \max\left\{\left(\lambda_w^v(i) + \alpha_i g_{\lambda_w^v}\right),\ 0\right\} \tag{31}$$

The Lagrange multipliers λ_s^{lm}, $\forall m \in \psi_l$ are then updated at link l using the primal solutions from all other link $m \in \psi_l$, that fall within its interference range, as follows:

$$\lambda_s^{lm}(i+1) = \lambda_s^{lm}(i) + \beta_i g_{\lambda_s^{lm}} \tag{32}$$

C. Obtaining Feasible Primal Solutions

The sequence of primal solutions that we get at every iteration of the subgradient method may not necessarily converge. Hence we use a convex combination of solutions obtained at every iteration, also referred to as the ergodic iterates [21]. The sequence of ergodic iterates is known to converge to the optimal solution set of the primal problem with relaxed integral constraints [19]. Specifically at every iteration, we use the s^2-rule, introduced by [19] to compute the convexity weights for the ergodic updates. Let i_{max} be the maximum number of iterations. Initialized as $\overline{x}_0 = x_0$, the ergodic iterate $\overline{x}_i$ of the primal variable x is updated at every iteration i, $\forall\, 1 \le i \le i_{max}$, as follows:

$$\overline{x}_i = \left(\overline{x}_{i-1}\sum_{s=1}^{i-1} s^2 + x_{i-1} i^2\right)\left(\sum_{s=1}^{i} s^2\right)^{-1} \tag{33}$$

The primal solutions thus obtained, converge to a near-feasible solution set of the relaxed primal problem [21]. But they are generally infeasible in the original problem. We then use heuristics to make adjustments to the latest iteration and construct a primal feasible solution in a distributed manner. w_l effectively represents the data flow on link l. Hence for every node v, the normalized ratio $w_l / \sum_{m \in \mathcal{O}_v} w_m$ is used to determine the fraction of outgoing traffic from node v that the link l would carry. Let w_l^c be the value of w_l computed in this manner. We use the link schedule variable s_l, directly from the solution set. With the values of s_l fixed, the constraints in Eqs. (15) and (16) directly give us an upper bound on the values of t_l. With w_l fixed at w_l^c, t_l is also lower bounded by the maximum possible transmit rate on a link. Let t_l^{lb} and t_l^{ub} be the lower and upper bounds on t_l. Now determining the most energy-efficient value of t_l boils down to locally solving the following minimization problem using standard methods:

$$\text{minimize} \quad \left[\tilde{\mathbb{P}}_l\left(\hat{r}_l\right) + \tilde{\log}\left(t_l\right)\right] \tag{34}$$

$$\text{subject to} \quad \hat{r}_l + \tilde{\log}\left(t_l\right) = \log\left(w_l^c\right) \tag{35}$$

$$t_l^{\text{lb}} \le t_l \le t_l^{\text{ub}} \tag{36}$$

Our decentralized delay-constrained energy-optimization approach is summarized in Algorithm 1.

Algorithm 1: Decentralized Co-Operative Algorithm

Initialize $(\boldsymbol{\lambda_w}, \boldsymbol{\lambda_s})^0 \leftarrow 0$
for $i = 1$ to i_{max} **do**
  for all links $l \in \mathcal{L}$ **do**
    compute $(w_l, s_l, t_l)^i$ Eqs. (24)-(28)
    share $(w_l, s_l, t_l)^i$ with concerned entities
    update ergodic iterates $\left(\overline{w_l}, \overline{s_l}, \overline{t_l}\right)^i$ Eq. (33)
  end for
  for all nodes $v \in \mathcal{V}$ **do**
    update $\left(\lambda_w^v\right)^i$ Eq. (31)
  end for
  for all links $l \in \mathcal{L}$ and $m \in \psi_l$ **do**
    update $\left(\lambda_s^{lm}\right)^i$ Eq. (32)
  end for
  if $\boldsymbol{\lambda_w}$ and $\boldsymbol{\lambda_s}$ haven't improved **then**
    break
  end if
end for
generate heuristic feasible solutions from $\left(\overline{\boldsymbol{w}}, \overline{\boldsymbol{s}}, \overline{\boldsymbol{t}}\right)$

VII. Performance Evaluation

We evaluate the performance of our decentralized delay-constrained energy optimization algorithm, against that of the centralized optimization approach. We further compare both their performance with that of the time-sensitive greedy forwarding (TGF) and time-sensitive least cost routing (TLCR) approaches as described in Sections VII-D.1 and VII-D.2 respectively. While the algorithms proposed in this paper are generic enough for use in any of the HLSNs, we focus on UWA-SN to analyze their performance since it has one of the most difficult communication media [9].

A. Performance Metrics

We use the following metrics to evaluate the performance of our algorithms.

1) Energy Cost Per Bit: Defined as the average energy cost incurred in delivering a bit of data from the sensors to the sinks. It is computed as the ratio of total energy consumed in the network to the total data delivered to the sinks in one TDMA frame.

2) Network Throughput: Defined as the average rate of successful delivery of data from all the sensors in the network to the sinks. It is computed as the ratio of the total data delivered to the sinks in one frame, to the TDMA time period.

B. Simulation Setup

We consider a UWA-SN model where a number of stationary sensor nodes are arbitrarily deployed with uniform distribution under the ocean in a 3D environment. The sink is placed at the center of the network. Results were captured for a varying number of sensor nodes. For every test with a given number of sensor nodes, results were averaged over multiple iterations. The location of the sensor nodes were changed in each of the iterations. Table II shows the values of different network parameters used in the tests.

We compare the performance of the algorithms for a fixed BER of 10^{-4}. Let ϵ be the required BER. For a given packet size of M bits, we approximate the expected number of transmissions on a link as $(1 + M\epsilon)$. In our simulations we adjust the network load contributed by each of the sensors to account for the expected number of retransmissions.

1) UWA-SN (UWA-SN): The available bandwidth of an underwater acoustic medium depends on both transmission range and frequency [22]. Signal attenuation due to absorption of acoustic energy, refractive properties of the medium and ambient noise from wind and shipping activity further deteriorate the link quality. The propagation delay in an underwater acoustic medium is not only large due to the slow speed of sound in water ($c_s \approx 1500\,\mathrm{m/s}$), but it also varies due to factors such as the temperature, pressure and salinity of

TABLE II
SIMULATION PARAMETERS

PARAMETER	VALUE
Network dimensions	10 x 10 x 0.2 km^3
Number of sensors	5 to 30
Max egress links per node	5
Sensor data per TDMA frame	20 kbit ($\pm 25\,\%$)
Max transmit power	182 dB re μPa
Carrier frequency	25 kHz
Bandwidth	1 kHz
Bit Error Rate	10^{-4}
Noise PSD	41 (dB re μPa) /Hz
Spreading factor	1.7
Packet size	32 bytes
Electric to acoustic loss	172 dBW re μPa
Relay processing power	0.05 W

the water. The underwater acoustic channel model used in this paper, accounts for the dependency of the path loss on the signal frequency, multi-path spread, path dispersion, propagation delay, and random channel variations including motion induced Doppler shifts as described in [4] and [23]. In our tests, we use the simulator developed by [23] to model the underwater acoustic channel. Given the frequency selective fading nature of the underwater acoustic channel, we use the frequency domain statistical water-filling power allocation method [24] to maximize channel capacity.

C. Performance Evaluation of the Proposed Algorithms

Fig.5 and Fig.6 show the average energy consumed per bit (in μJ) versus the total number of sensor nodes, for our centralized and decentralized approaches. Plots are shown for different time periods T. Our proposed algorithms generate interference-free overlapping schedules. As a result, an increase in the total network load has little impact on the energy consumed per bit until a certain point. The threshold occurs when there no longer exists a schedule that can accommodate the current network load without increasing the transmit power to achieve higher data rates. Once the load in the network crosses the said threshold, the energy consumed per bit begins to increase rapidly as expected. As the time period T is relaxed, the amount of load that the network can handle before it reaches the critical threshold, also increases. This is intuitively expected and is illustrated in Fig.5 and Fig.6.

With further increase in network load, after a certain point, feasible schedules do not exist anymore. This happens when the maximum TDMA time period is not large enough to accommodate the transmissions on all the links of any valid route-set. In such a scenario, the centralized solver will return an infeasible status and the solutions obtained with the decentralized approach will be infeasible as expected. The portion of the plots in Fig.6, where the curves begin to drop down after the peak, correspond to scenarios where solutions do not exist.

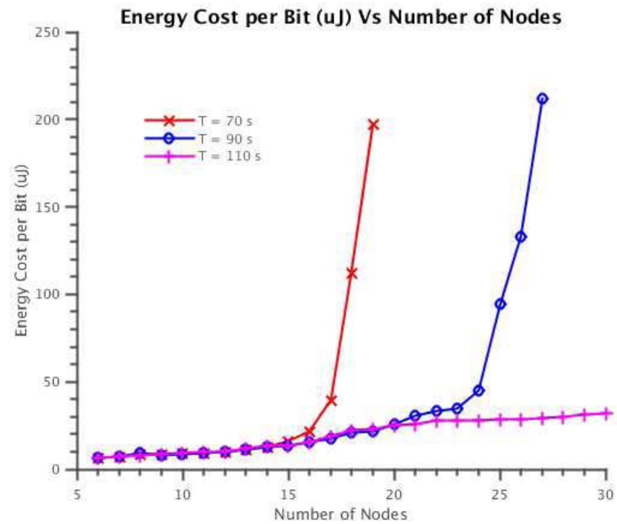

Fig. 5. Energy efficiency of the centralized approach for different maximum time periods. $\epsilon = 10^{-4}$.

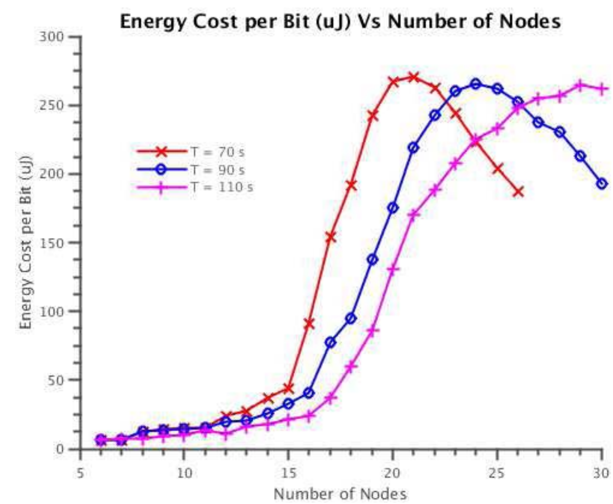

Fig. 6. Energy efficiency of the decentralized approach for different maximum time periods. $\epsilon = 10^{-4}$.

Fig.7 and Fig.8 show the network throughput (in bps) versus the total number of sensor nodes, for our centralized and decentralized approaches. Plots are shown for different time periods T. They demonstrate the ability of our proposed approaches to generate conflict-free overlapping schedules. As expected, we observe the overall network throughput increase with the network load and also with decreasing time periods. For a given network load, the TDMA time period, which is an input to our algorithms, can be adjusted to not only increase the throughput of the network, but also to minimize energy consumption.

D. Performance Comparison With Other Approaches

In this section we compare the performance of our proposed centralized and decentralized algorithms with the following two alternative approaches.

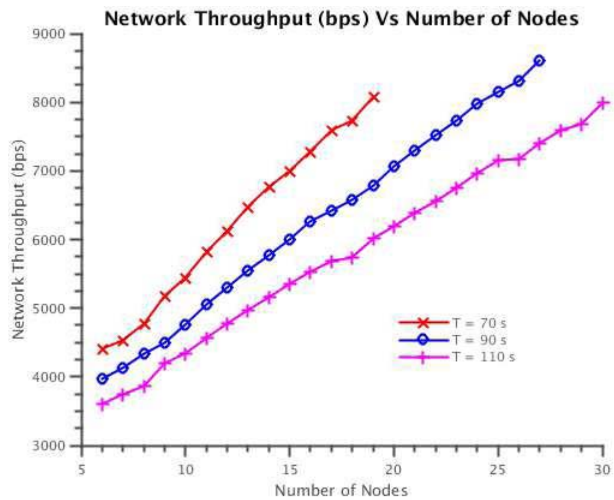

Fig. 7. Throughput efficiency of the centralized approach for different maximum time periods. $\epsilon = 10^{-4}$.

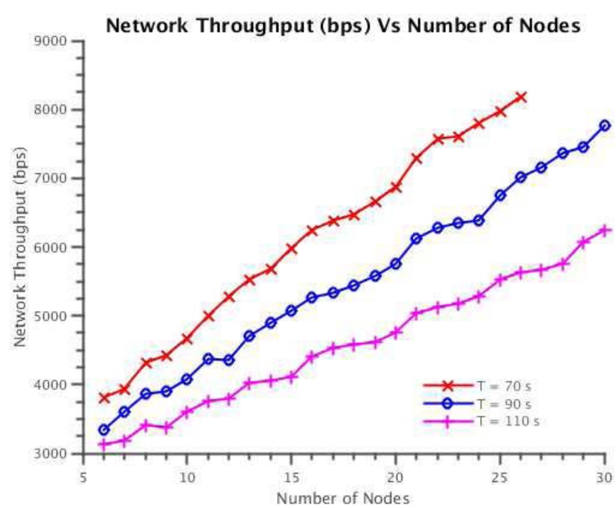

Fig. 8. Throughput efficiency of the decentralized approach for different maximum time periods. $\epsilon = 10^{-4}$.

1) TGF (TGF): Greedy forwarding is one of the most widely used localized routing methods. TGF is a modified version of the Greedy Minimum Energy forwarding algorithm described in [13], updated to handle global delay constraints. This modification helps us make more meaningful evaluations of our delay-constrained energy optimization algorithms. The TGF scheme exploits location information to make routing decisions. Every sensor node is allocated an equal number of time slots per frame. In addition to the signal transmission time, to avoid interference, the nodes also need to account for the propagation delay on the chosen outgoing link. The sensor nodes shortlist a finite number of next hop candidates that are closer to a sink than itself. The nodes then estimate the amount of energy required for transmission on each of the links, using as input the link propagation delays, number of time slots that are available for transmission, amount of incoming relay traffic and the amount of locally generated data per time period. They then select the link that consumes the least amount of energy.

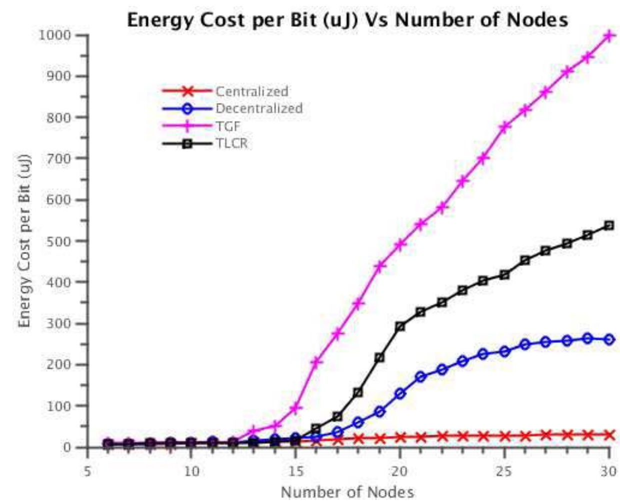

Fig. 9. Energy efficiency comparison between the proposed and alternative approaches. $\epsilon = 10^{-4}$, $T = 110\,\text{s}$.

2) TLCR (TLCR): Unlike TGF, TLCR is an offline routing algorithm. It is a modified version of the Centralized Optimum algorithm described in [13], updated to handle global delay constraints. In this scheme, the Dijkstra's algorithm is used to determine the least cost path from a sensor to the sink. The algorithm is run for each of the sensors, one sensor at a time, in decreasing order of its distance from the sink. At every iteration, the cost of each of the links in the network is updated based on the incremental energy required to transmit the data generated by the source sensor, on that link. Every sensor node is allocated an equal number of time slots per frame. The incremental energy cost for each of the links is computed based on the amount of data that the link is already carrying, the propagation delay for the link and the remaining number of time slots that are available for transmission at the source of the link.

E. Comparative Results

By design, the projected subgradient algorithm converges in an iterative manner. As the scale of the problem increases, the number of iterations required to obtain a near-optimal solution, also increases. In order to limit the amount of time and energy spent on computations, we use a predefined number of iterations i_{max} as one of our stopping criteria. As a result, we see in Fig.9 that the plot for the energy consumption with the decentralized algorithm diverges away from that of the optimal centralized solutions, as the number of nodes in the network increase. In small networks with relatively few relay sensors, the performance of TGF and TLCR are comparable to our proposed approaches. The performance gap begins to widen as the size of the network increases. We observe that while our decentralized algorithm takes a performance hit of ≈ 8 dB when compared to the centralized approach at capacity, it is nevertheless ≈ 6 dB and ≈ 3 dB more energy efficient than the TGF and TLCR algorithms respectively.

Fig.10 shows the network throughput (in bps) versus number of sensors for the centralized, decentralized, TGF and the TLCR algorithms. The TGF routes generally contain a greater number of hops than the TLCR routes. Hence the total time

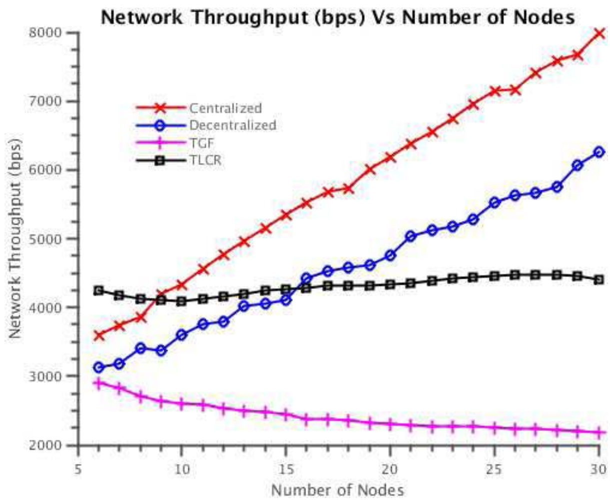

Fig. 10. Throughput efficiency comparison between the proposed and alternative approaches. $\epsilon = 10^{-4}$, $T = 110\,\text{s}$.

spent on signal propagation is larger for TGF. This translates to a smaller TDMA frame size and a higher network throughput for TLCR when compared to TGF.

When the centralized and decentralized algorithms are not constrained by time, the link schedules generated by them are spaced out, resulting in a low network throughput. But as network load increases, the proposed algorithms produce conflict-free overlapping schedules, thereby increasing the overall network throughput. This is illustrated in Fig.10 where the throughput scales with increasing load for both the centralized and decentralized approaches. We observe that while the decentralized approach is ≈ 1 dB less throughput-efficient than the centralized approach at capacity, it is still ≈ 5 dB and ≈ 2 dB more throughput-efficient than the TGF and TLCR algorithms respectively.

For all the discussed algorithms, simulations were also run for a BER of 10^{-6}, and the comparative results obtained were similar to those observed with a BER of 10^{-4}.

VIII. Conclusion

A mixed-integer programming (MIP) formulation of the delay-constrained energy optimization problem was considered to compute near-optimal routes, schedule and power control solutions for high-latency sensor network (HLSN). This approach allowed us to compute approximate solutions to an optimization problem that is otherwise difficult to solve. This difficulty is attributed to the lack of well-established closed-form analytical models for the high-latency media such as underwater acoustic and satellite-based long-range radio frequency channels. Further, a decomposition of the centralized optimization problem using Lagrangian multipliers was considered to solve the problem in a decentralized manner using the subgradient descent method. Comparative analysis was carried out using simulations to evaluate the performance of both the centralized and the decentralized approaches against the heuristic time-sensitive greedy forwarding (TGF) and time-sensitive least cost routing (TLCR) algorithms.

We have shown that our MIP-based energy optimization framework can be effectively used to generate near-optimal solutions for networks with complex channel characteristics. Our approach also increases the overall throughput of the network by taking advantage of the inherently large propagation delay of the medium to schedule conflict-free overlapping transmissions. Our simulation results show that both the centralized and decentralized algorithms outperform the TGF and TLCR approaches with respect to energy and throughput efficiency, by a wide margin. We observed that the performance gap between TGF, TLCR and our proposed algorithms widens with increasing network load. As the number of nodes in the network increases, the size and complexity of the centralized algorithm grows as well. Our decentralized approach on the other hand pays a reasonable performance penalty of $\approx$ 8 dB of energy-efficiency and $\approx$ 1 dB of throughput-efficiency when compared to our centralized approach, in exchange for better scalability.

Improving the speed of convergence of the distributed algorithm is a suggested area for future research. Being able to estimate the distance between the current and the optimal solution set in the subgradient algorithm can enable us to use Polyak step sizes that are known to converge faster [18, p. 2619]. This can be achieved by using a coordinator node to assimilate the results of the subproblems and compute the dual objective at each iteration. Finally, improving the quality of the solutions by using alternative heuristic primal recovery methods, could be another area of research interest.

Appendix
Solving Decentralized Subproblems

Here we discuss the implementation details of solving the decentralized link-specific optimization subproblem specified in Eq. (24). Since $e_l = p_l t_l$, we have: $\log(e_l) = \log(p_l) + \log(t_l)$.

Let $\mathbf{\Gamma_k}$ and $\mathbf{\Gamma_c}$ be two vectors that contain the knot and coefficient components respectively, of breakpoints that are used to approximate the log function. Let $\langle ., . \rangle$ denote an inner product expression of two vectors. If a variable x is replaced by a vector $\boldsymbol{\mathcal{S}}^{\boldsymbol{x}}$ of special ordered set type 2 (SOS2) variables [25] such that $\sum \boldsymbol{\mathcal{S}}^{\boldsymbol{x}} = 1$ and $x = \langle \mathbf{\Gamma_k}, \boldsymbol{\mathcal{S}}^{\boldsymbol{x}} \rangle$, then $\tilde{\log}(x)$ can be computed as $\tilde{\log}(x) = \langle \mathbf{\Gamma_c}, \boldsymbol{\mathcal{S}}^{\boldsymbol{x}} \rangle$. Let Υ_k and Υ_c be the knot and coefficient vectors of breakpoints used to approximate function $\mathbb{P}_l$.

Let $\boldsymbol{\mathcal{S}}_l^{\boldsymbol{e}}$, $\boldsymbol{\mathcal{S}}_l^{\boldsymbol{w}}$, $\boldsymbol{\mathcal{S}}_l^{\boldsymbol{t}}$ and $\boldsymbol{\mathcal{S}}_l^{\boldsymbol{p}}$, each be a vector of SOS2 variables such that $e_l = \langle \mathbf{\Gamma_k}, \boldsymbol{\mathcal{S}}_l^{\boldsymbol{e}} \rangle$, $w_l = \langle \mathbf{\Gamma_k}, \boldsymbol{\mathcal{S}}_l^{\boldsymbol{w}} \rangle$, $t_l = \langle \mathbf{\Gamma_k}, \boldsymbol{\mathcal{S}}_l^{\boldsymbol{t}} \rangle$ and $\hat{r}_l = \langle \Upsilon_k, \boldsymbol{\mathcal{S}}_l^{\boldsymbol{p}} \rangle$. We then have $\tilde{\mathbb{P}}_l(\hat{r}_l) = \langle \Upsilon_c, \boldsymbol{\mathcal{S}}_l^{\boldsymbol{p}} \rangle$. Since $r_l = w_l/t_l$, we have $\hat{r}_l = \log(w_l) - \log(t_l)$. The propagation time for link l is $\tau_l = d_l c_s$.

The decentralized MIP subproblem Eq. (24) for any link $l \in \mathcal{L}$, can now be modeled as follows:

$$\underset{s_l \geq 0}{\text{minimize}} \begin{bmatrix} \langle \mathbf{\Gamma_k}, \boldsymbol{\mathcal{S}}_l^{\boldsymbol{e}} \rangle \\ + \left(\lambda_w^{\mathrm{x}(l)} - \lambda_w^{\mathrm{r}(l)} \right) \langle \mathbf{\Gamma_k}, \boldsymbol{\mathcal{S}}_l^{\boldsymbol{w}} \rangle \\ + \left(\sum_{m \in \psi_l} \lambda_s^{lm} + \rho_l \right) \langle \mathbf{\Gamma_k}, \boldsymbol{\mathcal{S}}_l^{\boldsymbol{t}} \rangle \\ + \left(\sum_{m \in \psi_l} \left(\lambda_s^{lm} - \lambda_s^{ml} \right) \right) s_l \end{bmatrix} \tag{37}$$

$$\text{subject to} \quad s_l + \langle \mathbf{\Gamma}_k, \mathcal{S}_l^t \rangle \le T - \tau_{max} \tag{38}$$
$$\langle \Upsilon_k, \mathcal{S}_l^p \rangle = \langle \mathbf{\Gamma}_c, \mathcal{S}_l^w \rangle - \langle \mathbf{\Gamma}_c, \mathcal{S}_l^t \rangle \tag{39}$$
$$\langle \mathbf{\Gamma}_c, \mathcal{S}_l^e \rangle = \langle \Upsilon_c, \mathcal{S}_l^p \rangle + \langle \mathbf{\Gamma}_c, \mathcal{S}_l^t \rangle \tag{40}$$
$$\sum \mathcal{S}_l^e = 1 \quad \sum \mathcal{S}_l^w = 1$$
$$\sum \mathcal{S}_l^t = 1 \quad \sum \mathcal{S}_l^p = 1 \tag{41}$$

Constraints in Eq. (41) implicitly define bounds on their respective SOS2 variables. Since this subproblem only involves variables associated with one link, the size of the problem is very small. As a result, it can be effortlessly solved with any of the standard methods available for solving MIP problems.

REFERENCES

[1] M. Goetz and I. Nissen, "GUWMANET—Multicast routing in underwater acoustic networks," in *Proc. Military Commun. Inf. Syst. Conf. (MCC)*, Oct. 2012, pp. 1–8.

[2] W. Colitti, K. Steenhaut, N. Descouvemont, and A. Dunkels, "Satellite based wireless sensor networks: Global scale sensing with nano- and pico-satellites," in *Proc. 6th ACM Conf. Embedded Netw. Sensor Syst. (SenSys)*, New York, NY, USA, 2008, pp. 445–446.

[3] D. A. Jiraud, "LEO satellite channels for packet communications," *Appl. Microw. Wireless*, vol. 7, p. 42–55, 1995.

[4] M. Stojanovic, "On the relationship between capacity and distance in an underwater acoustic communication channel," *ACM SIGMOBILE Mobile Comput. Commun. Rev.*, vol. 11, no. 4, pp. 34–43, Oct. 2007. [Online]. Available: http://doi.acm.org/10.1145/1347364.1347373

[5] S. Cui, R. Madan, A. J. Goldsmith, and S. Lall, "Cross-layer energy and delay optimization in small-scale sensor networks," *IEEE Trans. Wireless Commun.*, vol. 6, no. 10, pp. 3688–3699, Oct. 2007.

[6] D. E. Lucani, M. Medard, and M. Stojanovic, "Underwater acoustic networks: Channel models and network coding based lower bound to transmission power for multicast," *IEEE J. Sel. Areas Commun.*, vol. 26, no. 9, pp. 1708–1719, Dec. 2008.

[7] P. Ponnavaikko, K. Yassin, S. K. Wilson, M. Stojanovic, and J. Holliday, "Energy optimization with delay constraints in underwater acoustic networks," in *Proc. IEEE Global Commun. Conf. (GLOBECOM)*, Dec. 2013, pp. 551–556. [Online]. Available: http://ieeexplore.ieee.org/stamp/stamp.jsp?arnumber=6831129

[8] G. Anastasi, M. Conti, M. Di Francesco, and A. Passarella, "Energy conservation in wireless sensor networks: A survey," *Ad Hoc Netw.*, vol. 7, no. 3, pp. 537–568, May 2009. [Online]. Available: http://dx.doi.org/10.1016/j.adhoc.2008.06.003

[9] M. Stojanovic, "Underwater acoustic communications: Design considerations on the physical layer," in *Proc. 5th Annu. Conf. Wireless Demand Netw. Syst. Services (WONS)*, 2008, pp. 1–10.

[10] M. K. Park and V. Rodoplu, "UWAN-MAC: An energy-efficient MAC protocol for underwater acoustic wireless sensor networks," *IEEE J. Ocean. Eng.*, vol. 32, no. 3, pp. 710–720, Jul. 2007.

[11] S. A. Samad, S. K. Shenoy, G. S. Kumar, and P. R. S. Pillai, "RMAC-M: Extending the R-MAC protocol for an energy efficient, delay tolerant underwater acoustic sensor network application with a mobile data mule node," in *Proc. Int. Symp. Ocean Electron. (SYMPOL)*, 2011, pp. 217–223.

[12] K. Kredo, II, and P. Mohapatra, "Scheduling granularity in underwater acoustic networks," in *Proc. 6th ACM Int. Workshop Underwater Netw. (WUWNet)*, New York, NY, USA, 2011, pp. 7:1–7:8. [Online]. Available: http://doi.acm.org/10.1145/2076569.2076576

[13] M. Zorzi, P. Casari, N. Baldo, and A. F. Harris, "Energy-efficient routing schemes for underwater acoustic networks," *IEEE J. Sel. Areas Commun.*, vol. 26, no. 9, pp. 1754–1766, Dec. 2008.

[14] D. Pompili, T. Melodia, and I. F. Akyildiz, "Routing algorithms for delay-insensitive and delay-sensitive applications in underwater sensor networks," in *Proc. 12th Annu. Int. Conf. Mobile Comput. Netw. (MobiCom)*, New York, NY, USA, 2006, pp. 298–309.

[15] F. A. de Souza, B. S. Chang, G. Brante, R. D. Souza, M. E. Pellenz, and F. Rosas, "Optimizing the number of hops and retransmissions for energy efficient multi-hop underwater acoustic communications," *IEEE Sensors J.*, vol. 16, no. 10, pp. 3927–3938, May 2016.

[16] L.-C. Kuo and T. Melodia, "Tier-based underwater acoustic routing for applications with reliability and delay constraints," in *Proc. IEEE Int. Workshop Wireless Mesh Ad Hoc Netw. (WiMAN)*, Maui, HI, USA, Jul. 2011, pp. 1–6.

[17] B. Benson *et al.*, "Design of a low-cost underwater acoustic modem," *IEEE Embedded Syst. Lett.*, vol. 2, no. 3, pp. 58–61, Sep. 2010.

[18] C. A. Floudas and P. M. Pardalos, *Encyclopedia of Optimization*, vol. 1. New York, NY, USA: Springer, 2008.

[19] E. Gustavsson, M. Patriksson, and A.-B. Strömberg, "Primal convergence from dual subgradient methods for convex optimization," *Math. Program.*, vol. 150, no. 2, pp. 365–390, May 2015. [Online]. Available: http://dx.doi.org/10.1007/s10107-014-0772-2

[20] M. Han, "Computational study of the step size parameter of the subgradient optimization method," Dept. Statist., Dalarna Univ., Falun, Sweden, Tech. Rep., 2013. [Online]. Available: http://www.diva-portal.org/smash/record.jsf?pid=diva2%3A658495

[21] P. Aldenvik, M. Schierscher, "Recovery of primal solutions from dual subgradient methods for mixed binary linear programming; A branch-and-bound approach," M.S. thesis, Dept. Math. Sci., Univ. Gothenburg, Gothenburg, Sweden, 2015. [Online]. Available: http://hdl.handle.net/2077/40726

[22] M. Stojanovic and J. Preisig, "Underwater acoustic communication channels: Propagation models and statistical characterization," *IEEE Commun. Mag.*, vol. 47, no. 1, pp. 84–89, Jan. 2009.

[23] P. Qarabaqi and M. Stojanovic, "Statistical characterization and computationally efficient modeling of a class of underwater acoustic communication channels," *IEEE J. Ocean. Eng.*, vol. 38, no. 4, pp. 701–717, Oct. 2013.

[24] Y. M. Aval, S. K. Wilson, and M. Stojanovic, "On the achievable rate of a class of acoustic channels and practical power allocation strategies for OFDM systems," *IEEE J. Ocean. Eng.*, vol. 40, no. 4, pp. 785–795, Oct. 2015.

[25] E. M. L. Beale and J. A. Tomlin, "Special facilities in a general mathematical programming system for non-convex problems using ordered sets of variables," in *Proc. 5th Int. Conf. Oper. Res.*, 1970, pp. 447–454.

Poongovan Ponnavaikko received the B.E. degree in electronics and communications engineering from the National Institute of Technology, India, in 1997, and the M.S. degree in telecommunications from the University of Colorado at Boulder in 2002. He is currently pursuing the Ph.D. degree with the Computer Engineering Department, Santa Clara University, CA, USA. He is also a Principal Engineer with Brocade Communications. His research interests include wireless sensor networks, distributed algorithms design, and network energy optimization.

Sarah Kate Wilson (F'12) received the A.B. (Hons.) degree in mathematics from Bryn Mawr College in 1979 and the Ph.D. degree in electrical engineering from Stanford University in 1994. She has worked in both industry and academia and has been a Visiting Professor with the Lulea University of Technology, the Royal Institute of Technology, Stockholm, and Stanford University. She is currently an Associate Professor of Electrical Engineering at Santa Clara University. She has served as an Associate Editor for the IEEE TRANSACTIONS ON WIRELESS COMMUNICATIONS, the IEEE COMMUNICATIONS LETTERS, and the IEEE TRANSACTIONS ON COMMUNICATIONS, and as Editor-in-Chief of the IEEE COMMUNICATIONS LETTERS. Her research interests include orthogonal frequency division multiplexing and optical wireless communications. She was a former Director of Journals for the IEEE Communications Society.

Milica Stojanovic (F'10) graduated from the University of Belgrade, Serbia, in 1988, and received the M.S. and Ph.D. degrees in electrical engineering from Northeastern University, Boston, MA, USA, in 1991 and 1993, respectively. She was a Principal Scientist with the Massachusetts Institute of Technology until 2008, when she joined Northeastern University, where she is currently a Professor of Electrical and Computer Engineering. She is also a Guest Investigator at the Woods Hole Oceanographic Institution, and a Visiting Scientist at MIT. Her research interests include digital communications theory, statistical signal processing and wireless networks, and their applications to underwater acoustic systems. She is currently Associate Editor of the IEEE JOURNAL OF OCEANIC ENGINEERING, Associate Editor of the IEEE TRANSACTIONS ON SIGNAL PROCESSING, Chair of the IEEE Ocean Engineering Society's Technical Committee for Underwater Communications, Advisory Board Member of the IEEE COMMUNICATION LETTERS, and Editorial Board Member of the Elsevier *Physical Communication Journal*.

JoAnne Holliday received the B.S. degree in physics from the University of California, the M.S. degree from Northeastern University, and the Ph.D. degree in computer science from the University of California at Santa Barbara in 2000. She joined the Faculty at Santa Clara University in 2000, where she is currently a tenured Associate Professor of Computer Engineering. Her research involves maintaining consistency in distributed systems and devising new energy efficient algorithms for ad-hoc and sensor networks. Her recent interests include peer-to-peer networks and wireless 802.11 and cellular technology. She is currently serving as an Associate Editor of the IEEE COMMUNICATIONS LETTERS.

Kamal Yassin received the B.S. degree in electrical engineering from the University of Jordan in 1999 and the M.S. degree in electrical and computer engineering from the University of North Carolina at Charlotte in 2000. He is currently pursuing the M.B.A. degree with the University of Illinois at Urbana–Champaign. He is currently a Director of Product Management at ASSIA, Inc., California. His research interests include wireless networks, specifically, quality of experience in wireless networks, self-healing networks, WiFi offload management, self-organizing networks, and radio resource management.